Proceedings of Ninth World Conference on Earthquake Engineering
August 2-9, 1988, Tokyo-Kyoto, JAPAN (Vol.VIII)

SA-1

THE INFLUENCE OF STRONG SOIL INHOMOGENEITY AND DISSIPATION ON GROUND MOTION

A. K. Mal and P.-C. Xu

Mechanical, Aerospace and Nuclear Engineering Department
University of California, Los Angeles
California 90024, U. S. A.

SUMMARY

The influence of strong soil inhomogeneity on earthquake ground motion is examined through theoretical modeling. A typical deposit is represented by a stack of homogeneous layers of dissipative viscoelastic material and the motion is produced by a line source. Calculations are carried out by means of a recently developed theoretical technique. The near surface low velocity layers are found to have a very strong amplification effect on the ground motion at some frequencies. The widely used one dimensional approach for site effect evaluation is shown to be valid for smaller epicentral distances only. The deamplification effect of material dissipation is shown to be extremely important in most cases.

INTRODUCTION

The prediction of certain properties (e. g., amplitude, duration and frequency content) of the expected earthquake ground motion at a given site in a seismically active region is of great importance in developing earthquake resistant design codes and criteria for the region. These characteristics are known to be influenced by a variety of factors which include the rupture process at the source, the distance and geologic properties of the earth material between the source and the site and the properties of the soil in the vicinity of the site. Among these factors, local soil conditions appear to have a strong influence on the relevant characteristics of ground motion in the entire range of distances where the shaking is relatively intense and where its frequency content covers the frequency range of engineering interest. Analysis of historical earthquake records, nuclear explosion data (Refs. 1, 2) and microtremor measurements (Ref. 3) have given some insight into the nature of this influence. However, a quantitative understanding of the phenomenon is lacking at present. Some of the specific issues which need to be carefully investigated can be stated as follows.

1. Most soil deposits exhibit a strong velocity gradient with depth near the free surface. The influence of this on the properties of ground motion is not well understood at present.

2. The tradeoff between the deamplification caused by the dissipative properties of the soil and the amplification due to wave trapping is widely recognized but the extent of the tradeoff is not well known.

3. The location of the source must be a significant factor, but this also needs clarification.

In this paper, we examine a deposit whose lateral dimensions are large compared to the depth and present calculations to determine the relative influence of its depth and material properties as well as of the source location on the resulting motion.

THEORETICAL MODEL

The stratified sediment is modeled by N homogeneous layers and the basement complex by a uniform half space. This representation seems to be justified by the available subsurface data in many deposit sites. In most cases, the shear wave velocity increases very rapidly within the top 300 meters or so and the depth of the sedimentary rocks is about 1 km.

The geometry of the layered medium is shown in Fig. 1 together with a coordinate system (x, y, z). The m -th layer ($m \leq N+1$) is assumed to be bounded by the planes $z = z_{m-1}$ and $z = z_m$; its material properties are denoted by $\rho(m), c_1(m), c_2(m)$, and the dissipation "quality factors" by $q_1(m)$ and $q_2(m)$ for the P- and S- waves, respectively. The complex wave numbers, $k_1(m)$, $k_2(m)$ and the complex elastic constants $\lambda(m), \mu(m)$ are related to these parameters through,

$$k_\alpha(m) = (1 + 0.5i/q_\alpha(m))\omega/c_\alpha(m) \qquad \alpha = 1, 2 \tag{1}$$

$$\mu(m) = \rho(m)c_2^2(m) / (1 + 0.5i/q_2(m))^2 \qquad \lambda(m) + 2\mu(m) = \rho(m)c_1^2(m) / (1 + 0.5i/q_1(m))^2 \tag{2}$$

where ω is the circular frequency. The source is assumed to be a time harmonic line force, so that the motion is independent of y and its time dependence is $\exp(-i\omega t)$. The relevant displacement and stress components at any point in the medium are denoted by u, w, τ_{xz} and σ_{zz}.

Following the usual procedure (Ref. 4, 5), a four dimensional vector is defined through the equation,

$$\{s(z)\} = \{\{u\ w\}\ \{\tau_{xz}\ \sigma_{zz}\}\} = \int_{-\infty}^{\infty} \{U(z)\ T(z)\}\ e^{ik(x-\xi)-i\omega t} dk \tag{3}$$

where ξ is the x coordinate of the source and the dependence of $\{U(z)\ T(z)\}$ on k and ω has been suppressed.

In general, {U T} in the m -th layer may be expressed in the form

$$\begin{Bmatrix} U(z) \\ T(z) \end{Bmatrix} = \begin{bmatrix} Q_a(m) & Q_b(m) \\ Q_c(m) & Q_d(m) \end{bmatrix} [E(z, m)] \begin{Bmatrix} C^+(m) \\ C^-(m) \end{Bmatrix} \tag{4}$$

where $\{C^+\}$ and $\{C^-\}$ are unknown two-dimensional constant vectors corresponding to the the downgoing and upgoing waves, respectively. The matrices which appear in (4) have been defined in Ref. 5.

The jump in the displacement-stress vector across the interface between the m -th and (m + 1) -th layers is given by

$$\begin{Bmatrix} U_-^+(m) \\ T_-^+(m) \end{Bmatrix} = \begin{bmatrix} Q_a(m+1)\ Q_b(m+1)E(m+1) \\ Q_c(m+1)\ Q_d(m+1)E(m+1) \end{bmatrix} \begin{Bmatrix} C^+(m+1) \\ C^-(m+1) \end{Bmatrix} - \begin{bmatrix} Q_a(m)E(m)\ Q_b(m) \\ Q_c(m)E(m)\ Q_d(m) \end{bmatrix} \begin{Bmatrix} C^+(m) \\ C^-(m) \end{Bmatrix} \tag{5a}$$

In absence of any interface feature,

$$\{U_-^+(m)\ T_-^+(m)\} = \{0\} \tag{5b}$$

Application of the interface conditions (5b), boundary conditions at $z = z_0$ and the radiation condition in the half space $z \geq z_N$ leads to the system of equations:

$$[Q]\{C\} = \{B\} \tag{6}$$

where

$$\{C\} = \{C^+(1)\ C^-(1)\ \ldots C^+(N)\ C^-(N)\ C^+(N+1)\}$$

$$\{B\} = \{T(z_0)\ 0\ \ldots 0\}$$

and [Q] is a (4N+2) x (4N+2) matrix composed of 2 x 2 submatrices.

Upon solving for {C}, the displacement-stress vector at any field point is obtained from (3) and (4). For a realistic model, the integral in (3) must be evaluated numerically and a series of computational difficulties must be overcome. We have been successful in developing an accurate and efficient numerical method for such a task. The details of this can be found in Refs. 4 and 6. The computer code based on the above mentioned theory generates the displacement and stress components to any desired degree of accuracy independent of the number of layers, total layer thickness, frequency range, or the location of the source and the stations. The program can be executed either on a mainframe or on an IBM PC. The number of function evaluations needed for each frequency point is in the range of 100-400. For the 8-layered structure of Fig. 1, the average computing time for the integrated displacement-stress vector per frequency point is about 7 minutes on an IBM PC/AT with 8 MHz clock speed or about 2.5 seconds CPU time on an IBM 3090 mainframe. The accuracy of the code has been tested through comparison of obtained results with other available ones (Ref. 7).

NUMERICAL RESULTS AND CONCLUSIONS

In the following, we consider a layered half space (Fig. 1) which represents a typical sedimentary structure in southern California (referred to as the UCLA site). We also consider a uniform half space which is identical to the bottom half space of the layered structure. The material properties are given in Table 1. In all cases, the unit line force is in the x direction, the unit dislocation is inplane shear in the x direction and the response is in the x direction. The term "relative displacement" is defined as the displacement on the surface of the layered half space or uniform half space divided by the epicentral displacement on the surface of the uniform half space due to the same source.

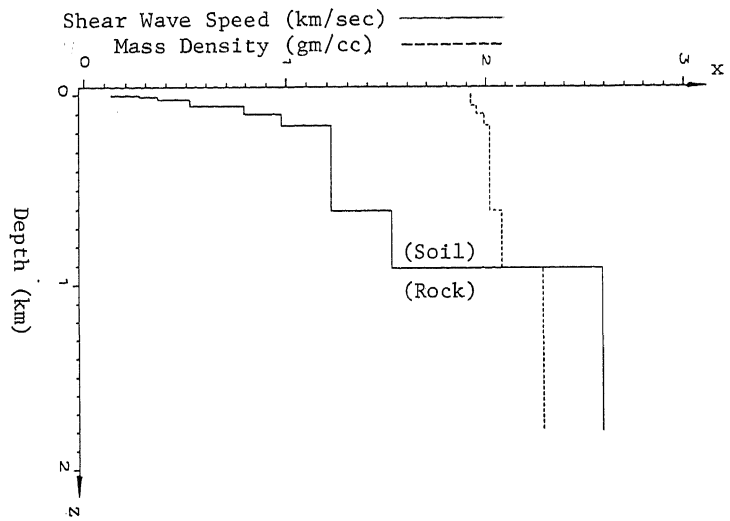

Fig. 1 Geometry and Material Properties of the "UCLA Site".

We have found from numerical tests that depth dependent (as given in Table 1) and constant (averaged values from the table) dissipation properties do not

produce a substantial difference in the results, at least in the frequency and distance ranges considered here. Hence, we have assumed constant attenuation ($q_1 = 68$ and $q_2 = 40$) in the top layers for all of the dissipative cases.

Fig. 2 shows the amplitude spectra of relative displacements on the surface of the layered half space without dissipation (top lines) and with dissipation (bottom lines) due to an impulsive line source located at (0 km, 5 km). The epicentral distances of the stations are 0, 5, 10, 20 km, respectively. As expected, at the epicenter, the result is identical to that for a normally incident plane wave, since the plane waves radiating from the source are all canceled out except in the normal direction. In the dissipative cases the spectra are depressed, but not evenly. The reduction is more significant at high frequencies, including resonant ones, and at the crests.

Table 1 UCLA SITE SUBSTRUCTURE

	Thickness (km)	Density (g/cm³)	c_1 (km/s)	c_2 (km/s)	Nondissipative q_1	Nondissipative q_2	Dissipative q_1	Dissipative q_2
1	0.0031	1.92	0.232	0.134	520	300	17	10
2	0.0067	1.92	0.465	0.268	520	300	34	20
3	0.0134	1.92	0.618	0.357	520	300	52	30
4	0.0354	1.92	0.898	0.518	520	300	68	40
5	0.0427	1.95	1.370	0.793	520	300	87	50
6	0.0610	1.95	1.690	0.975	520	300	102	60
7	0.4470	2.02	2.110	1.220	520	300	136	80
8	0.3050	2.08	2.640	1.520	520	300	170	100
9	Infinity	2.23	4.490	2.590	520	300	520	300

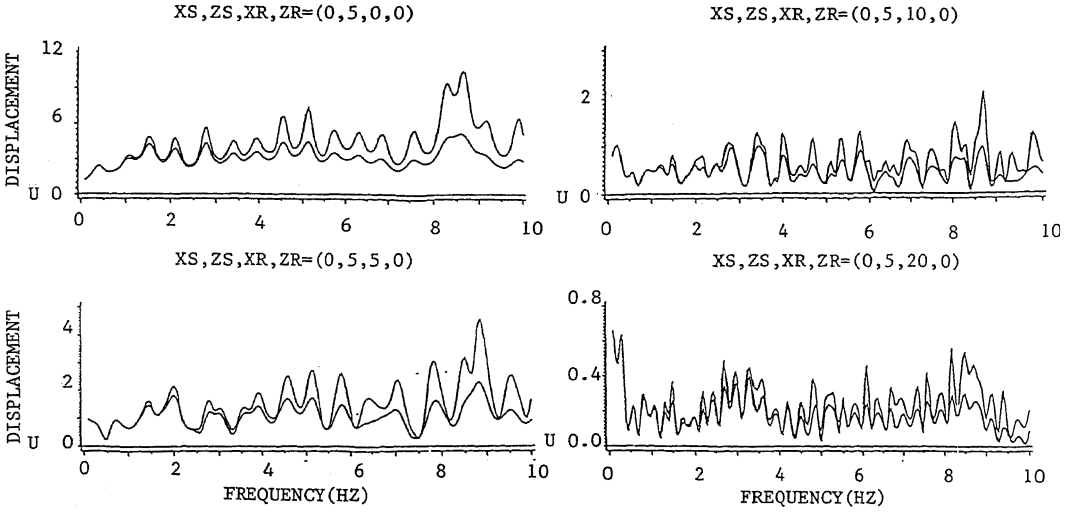

Fig. 2 Amplitude Spectra of Dissipative and Nondissipative Relative Displacements on the Surface.

The amplification effect of the soft layers and the deamplification effect of dissipation are illustrated in Fig. 3 where the top lines are the amplitude spec-

tra of displacements on the surface and bottom lines are those at 1 km depth in the layered half space due to an impulsive line source located at (0 km, 5 km). The left column is the nondissipative case and the right column is the dissipative case. The epicentral distances of the station pairs are 0, 5 and 10 km. In general, for stations embedded below the soft layers, the amplitude envelopes are reduced by a factor of about 5, compared to those of the corresponding surface stations. In addition, the resonance-related peaks disappear and the spectra become more even throughout the entire frequency range as in the uniform half space case. In all the spectra of Figs. 2 and 3 and especially for those at the epicenter, very large peaks arise at certain frequencies, e.g., around 8-9 Hz and 4-5 Hz. These are probably caused by the resonant response of the top two sedimentary layers.

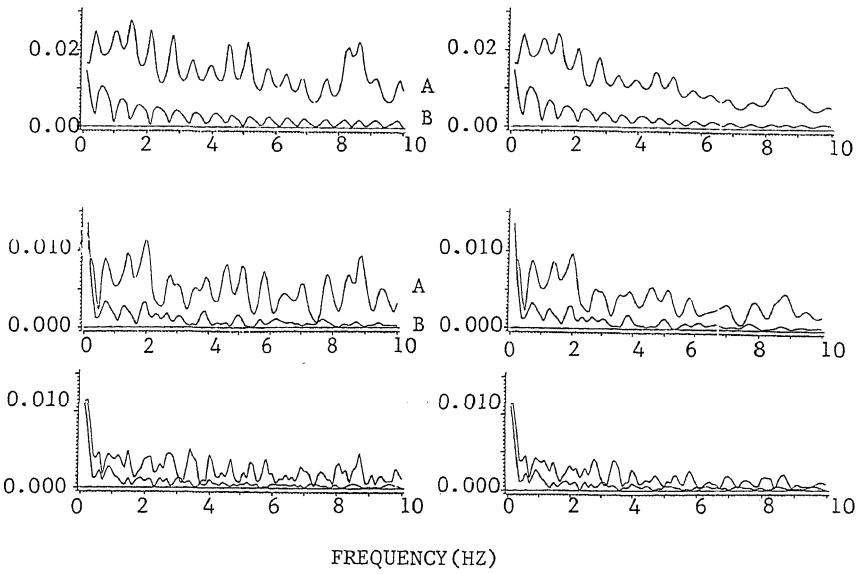

Fig. 3 Amplitude Spectra of Displacements on the Surface and at Depth.

For a station at larger epicentral distance, the main profile of the spectrum is preserved (Figs. 2, 3), but some minor oscillations are added. As expected, the magnitude of the whole spectrum is reduced nearly uniformly. It is noted that within a given frequency range, a fewer number of dominant resonant frequencies with wider effective range are replaced by a larger number of resonant frequencies with narrower effective range when the epicentral distance is increased.

The above mentioned features remain for sources at other depths as well as for dislocation sources. The response decays with source depth very rapidly. These results are not shown here due to space limitation.

The time histories of the ground acceleration due to a line source at 5 km depth for both the UCLA site (solid lines) and the uniform half space (dashed lines) are shown in Fig. 4. The slip function of the line source is assumed to be the modulated ramp with rise time 0.2 seconds, hence the predominant frequency of the source is 5 Hz. The epicentral distances are 0, 5, 10, 20 km, respectively. These results indicate that at smaller epicentral distances, the amplification of the peak acceleration is about 2.5-3 while at large epicentral distances, the effect of amplification of the soft soil is offset by deamplification due to dissipation. As expected, the sedimentary layers delay and multiply the P-, S- and Rayleigh wave pulses and prolong the duration of the ground motion.

In conclusion, our theoretical calculations show that the sedimentary layers have very strong amplification effects on the ground motion. The resonance pattern can be estimated properly by assuming normally incident plane wave if the station is at the epicenter. For stations at larger epicentral distances, the plane wave model is oversimplified. The deamplification of the spectra as well as the significant reduction in the resonant peaks caused by material dissipation are also important and should be considered in engineering applications.

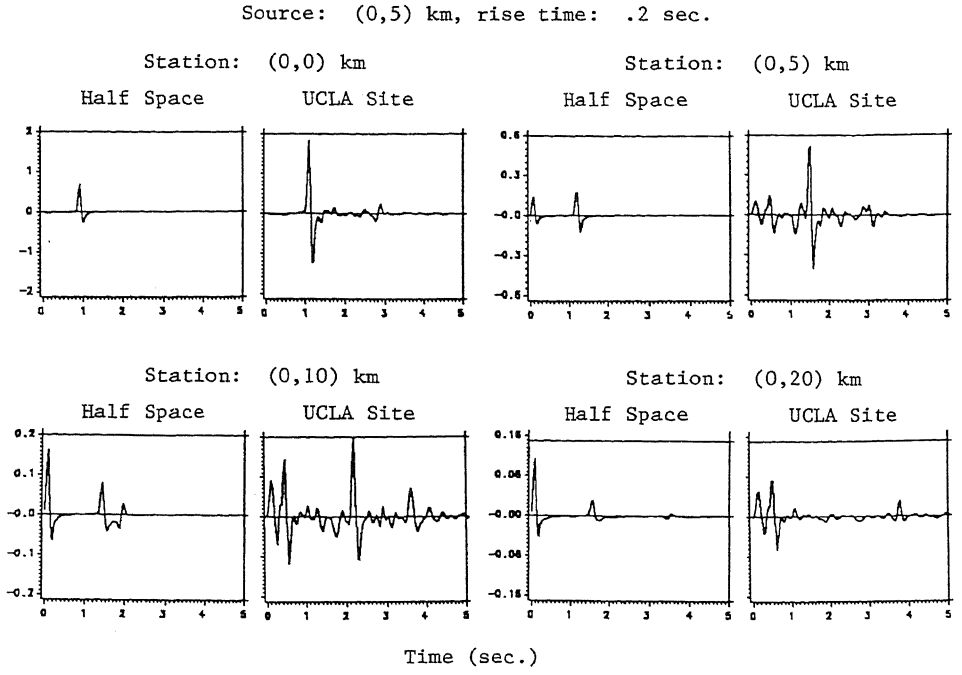

Fig. 4 Time Histories of the Ground Acceleration.

REFERENCES

1. Rogers, A. M., Tinsley, J. C. and Borcherdt, R. D., "Predicting Relative Ground Response, Evaluating Earthquake Hazards in the Los Angeles Region - An Earth-Science Perspective", U. S. Geological Survey Professional Paper, 1360, 221-248 (1985).
2. Tucker, B. E. and King, J. L., "Dependence of Sediment-filled Valley Response on the Input Amplitude and the Valley Properties", Bull. Seism. Soc. Am., 74, 153-165 (1984).
3. Kagami, H., Okada, S., Shiono, S., Oner, M., Dravinski, M. and Mal, A. K., "Observation of 1 to 5 Second Microtremors and their Application to Earthquake Engineering, Part III. A Two Dimensional Study of Site Effects in the San Fernando Valley", Bull. Seism. Soc. Am., 76, 1801-1812 (1986).
4. Xu, P.-C. and Mal, A. K., "Calculation of the In-plane Green's Functions for a Multilayered Viscoelastic Solid", Bull. Seism. Soc. Am., 77, 1823-1837 (1987).
5. Mal, A. K., "Guided Waves in Layered Solids with Interface Zones", Int. J. Eng. Sci. (1988, in press).
6. Xu, P.-C. and Mal, A. K., "An Adaptive Integration Scheme for Irregularly Oscillatory Functions", Wave Motion, 7, 235-243 (1985).
7. Xu, P.-C., Calculation of the Dynamic Green's Functions for Layered Viscoelastic Solids and their Applications Ph. D. dissertation, University of California, Los Angeles (1987).